Int. J. Electrochem. Sci., 16 **(2021)** Article Number: 211024, doi: 10.20964/2021.10.19

International Journal of ELECTROCHEMICAL SCIENCE
www.electrochemsci.org

Electrochemical Determination of Diclofenac Sodium in Pharmaceutical Sample Using Copper Nanoparticles/Reduced Graphene Oxide Modified Glassy Carbon Electrode

Haichi Yu[*], *Jianhang Jiao, Qiuju Li, Yingzhi Li*

Department of Orthopaedics, The Second Hospital of Jilin University, Changchun, 300041, China
[*]E-mail: liyingzhi2014@126.com

Received: 29 May 2021/ *Accepted:* 27 July 2021 / *Published:* 10 September 2021

This study presents electrochemical determination of diclofenac sodium (DCS) in a pharmaceutical sample using copper nanoparticles reduced graphene oxide hybrid electrodes (Cu NPs/rGO). rGOnanosheets were synthesized on a glassy carbon electrode (GCE) by modified Hummers method, and then, Cu NPs were electrodeposited on rGO/GCE. Results of structure and morphology studies by SEM and XRD revealed that the irregular Cu NPs electrodeposited in crystal structure with approximately 130nm diameter. Electrochemical analyses using the CV technique showed that Cu NPs/rGO/GCE exhibited a higher sensitivity for determination of DCS than that GCE, rGO/GCE and Cu NPs/GCE due to synergetic effect of Cu NPs and rGO which facilitates the electron transfer between the electrode and the electroactive species in solution and improve electrocatalytic oxidation of DCS. Amperometry measurements on Cu NPs/rGO/GCE as DCS sensor showed that linear range, limit of detection and sensitivity were obtained 20 to 400 µM, 8nM and 0.0356µA/µM, respectively. The applicability of Cu NPs/rGO/GCE to determine DCS concentration in the prepared real pharmaceutical sample was examined and results showed that recovery (≥97.66%) and RSD (≤3.05%) values were acceptable and this method provided suitable precision and accuracy for practical analyses in the pharmaceutical samples using Cu NPs/rGO/GCE.

Keywords: Diclofenac Sodium; Electrodeposition; Copper Nanoparticles; Reduced Graphene Oxide; Amperomety

1. INTRODUCTION

Diclofenac sodium (DCS) is the sodium salt form of diclofenac (2[2,6dichlorophenylamino]phenylacetic acid), a benzene acetic acid derivate and belongs to a class of drugs known as nonsteroidal anti-inflammatory drugs [1, 2]. This medicine works by reducing substances in the body that cause pain and inflammation [3, 4]. The analgesic, anti-inflammatory and

antipyretic activities of DCS make it as an effective drug for the treatment of acute, chronic pain and inflammatory and pain management in cases of kidney stones and gallstones, gout, arthritis, polymyositis, dermatomyositis, osteoarthritis, dental pain, temporomandibular joint pain, spondylarthritis, ankylosing spondylitis [5, 6].

Diclofenac side effects include vomiting, diarrhea, gastrointestinal bleeding, nausea, dizziness, headache, and swelling [7, 8]. Diclofenac can increase the risk of fatal heart attack or stroke, especially for long-term use or take high doses, or heart disease [9, 10]. Thus, determination of DCS dose is an important factor for pharmaceutical products such as oral tablets and capsules, eye drops, powder packets for oral solution [11, 12]. Therefore, many studies have been conducted to determine the DCS in pharmaceutical samples such as spectrophotometry, spectrofluorimetry, high-performance liquid chromatography, gas chromatography-mass spectrometry, polarography and electrochemical analyses [13-17].

Electrochemical analyses as the relatively inexpensive techniques can be optimized and miniaturized through micro- and nanostructured materials [18, 19]. Nanofabrication techniques can also be used to promote the performance of electrochemical sensors with providing the higher surface area and facilitate the electron transfer on electrode surfaces [20, 21]. Therefore, this study presents electrochemical determination of DCS in pharmaceutical sample using Cu NPs/rGO/GCE.

2. MATERIALS AND METHOD

2.1. Synthesis of CuNPs/rGO/GCE

Prior to the modification, the GCE surface was polished with 0.3 µm alumina slurry (99%, Sigma-Aldrich) followed by 0.05 µm alumina slurry on a wet polishing cloth to a mirror-like surface. Thereafter, the polished GCE was ultrasonically washed in ethanol and deionized water for 5 minutes in sequence, followed by drying under at room temperature.

In first step the rGO was synthesized by the modified Hummers method [22]. Briefly, 7 g graphite powder (99%, Qingdao Furuite Graphite Co., Ltd., China) were ball milled for 120 minutes to peel off graphene nanosheets from graphite because of weakening the van der Waals bonding between the graphite layers [22]. Next, the ball-milled powder was added into a beaker filled with 250 ml H_2SO_4 (98%, Merck, Germany) under stirring in an ice bath for 60 minutes. Subsequently, 35g $KMnO_4$ (99%, Henan Yongzhikun Water Treatment Materials Co., Ltd., China) was added to the beaker, and to complete the oxidation reaction and obtain the homogeneous dark brown solution. Then, 120 ml deionized water was ultrasonically added to the solution and it was sonicated for 6 hours at 35^oC. After then, the mixture was heated at 85^oC for 60minutes.After then, the reaction was stopped by addition 35 ml H_2O_2 (30%, Sigma-Aldrich). The resultant suspension was washed by HCl (37%, Merck, Germany) and deionized water, respectively. The obtained GO suspension was centrifuged at 2000 rpm for 30 minutes. For reduction of GO, 100 g/l L-ascorbic acid (99%, Sigma-Aldrich) solution as a reducing agent was added to centrifuge GO. Afterward, the mixture was heated at 90^oC for 80 minutes, and immediately was sonicated for 20 minutes at room temperature. The obtained rGO was centrifuged at 1000 rpm for 30 minutes and further was washed with 1M HCl solution and deionized water,

respectively. Finally, the obtained rGO suspension was dropped-coating on the GCE surface and dried at room temperature.

In second step, the Cu NPs were electrodeposited on the GCE and rGO/GCE using an Auto lab electrochemical analysis system (AUTOLAB PGSTAT 30, Eco Chemie B.V., Utrecht, The Netherlands) in a three electrode system containing an Ag/AgCl (3 M KCl) as the reference electrode, a platinum wire as counter electrode and GCE or rGO/GCE as working electrode through cyclic voltammetry (CV) technique. As a brief, the GCE or rGO/GCE was immersed into the deoxygenated 0.1 Na_2SO_4pH 7.0 containing 50mM $Cu(NO_3)_2$ (99%, Merck Germany) solution as an electrochemical electrolyte. The CV scanning was applied under the potential range between –0.5 V to 0.8 V at a scan rate of 50mV/s for sixty cycles.

2.2. Preparation of real samples

Diclofenac tablets were purchased from a local pharmacy which labeled with the amount of 25 mg per tablet.10 tablets (25 mg diclofenac) were finely powdered in a mortar and were ultrasonically dissolved in 25 ml of 0.1 M Na_2SO_4(99%, WeifangChangs Chemical Industry Co., Ltd., China), thereby the resulted solution with 1 mg/ml diclofenac content used as an electrolyte in an electrochemical cell. Then, the amperometry measurement at a potential of 0.41 V under successive addition of 2 mg/ml DCS has applied to determine the initial diclofenac in the prepared real pharmaceutical sample. The standard addition of DCS was used to determination of recovery and relative standard deviation (RSD).

2.3. Characterization

CV and amperometry measurements were carried out using Auto lab electrochemical analysis system. Prepared electrodes were used as a working electrode in electrochemical cell and 0.1 M $Na_2SO_4$was used as electrolyte for electrochemical studies. Scanning electron microscopy (SEM; S-3400, Hitachi, Tokyo, Japan) and X-ray diffraction (XRD; Rigaku D/MAX-2500/PC, Japan)) analyses were used to study the structural and surface morphologies of the prepared electrodes.

3. RESULT AND DISCUSSION

Figure 1 depicts SEM images of rGO/GCE, Cu NPs/GCE and Cu NPs/rGO/GCE. The SEM image in Figure 1a shows the pore structure of rGO with the typical ripples, folds and wrinkled nanosheets. As seen, a considerable amount of local accumulation between rGO nanosheets interfaces might be formed in the reduction process which can eliminate most of the oxygen-containing groups and sp^3 carbon [23]. It can generate more restacking of rGO nanosheets under π-π interaction [24]. Figure 1b shows the morphology of Cu NPs/GCE that exhibits the irregular nanoparticle with an approximate diameter of 175nm electrodeposited on GCE. The morphology of Cu NPs/rGO/GCE Figure 1c reveals deposition of Cu NPs with good dispersion on the surface of rGO nanosheets. The

average diameter of CuNPs is ~130nm. Comparison of Figures 1b and 1c displays that the electrodeposited Cu NPs are much smaller in size and lower aggregated in the presence of the rGO and large grains of nanoparticle are observed on the surface of GCE which indicated to the more electroactive and absorption sites on Cu NPs/rGO/GCE and it improves the active surface area and electron transfer activity in electrochemical cells. Moreover, the introduction of Cu NPs can reduce the agglomeration of rGO nanosheets which caused the higher electrochemical activity Cu of NPs/rGO/GCE.

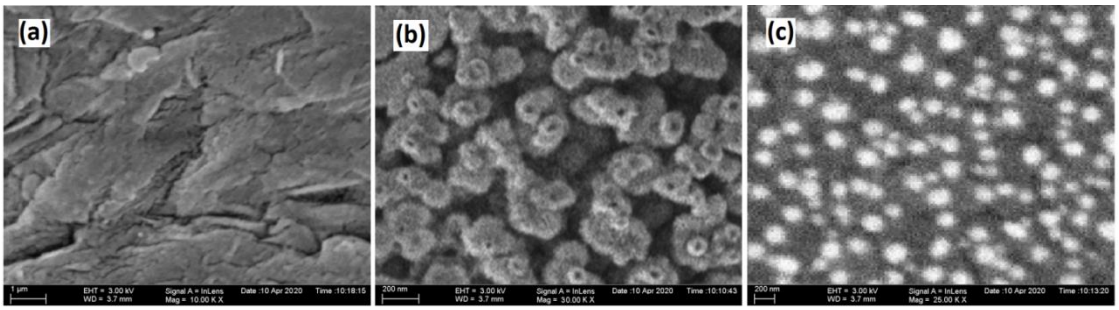

Figure 1. SEM images of (a) rGO/GCE, (b) Cu NPs/GCE and (c) Cu NPs/rGO/GCE.

Figure 2 shows XRD patterns of powders of rGO, Cu NPs and Cu NPs/rGO. The XRD pattern of rGO in Figure 2a shows a broad diffraction peak at 24.2° that it is related to (002) graphitic crystal plane. Figure 2b shows the XRD pattern of Cu NPs with diffraction peaks at 43.4°, 50.07° and 74.7° which are correlating to (111), (200) and (220) planes of the cubic structure of Cu, respectively (JCPDS card No. 04-0836). Figure 2c shows all of the diffraction peaks of (111), (200) and (220) of Cu and peak of (002) of rGO which indicated to maintaining the crystal structures of Cu NPs and rGO over the electrodeposition process.

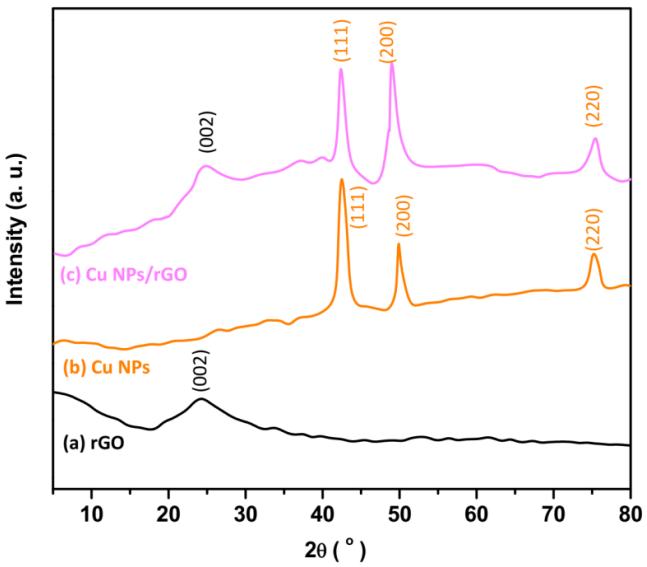

Figure 2. XRD patterns of powders of (a) rGO, (b) Cu NPs and (c) Cu NPs/rGO.

Figure 3a shows the CV curves of GCE, rGO/GCE, Cu NPs/GCE and Cu NPs/rGO/GCE in 0.1 M Na_2SO_4 pH 7 at scanning rate of 10mV/s. As seen from Figure 3a, the CV curves of GCE and rGO/GCE do not show any redox peaks. The CV curves of Cu NPs/GCE and Cu NPs/rGO/GCE show the anodic peaks (I) at 0.49 V and 0.42 V which attributed to oxidation of Cu_2O or CuOH to CuO, and the cathodic peaks (II) at 0.35 V and 0.37V which is related to the reduction of CuO into Cu_2O [25, 26]. The mechanism of the electrochemical redox is shown below [27]:

$Cu + OH^- \leftrightarrow CuOH + e^-$ (1)

$2CuOH \leftrightarrow Cu_2O + H2O$ (2)

$Cu_2O + 2OH^- \leftrightarrow 2CuO + H_2O + 2e^-$ (3)

The Cu nanoparticle was electrodeposited on GCE and rGO/GCE and further exposure Cu atoms in the surface of nanoparticles eventually became oxidized (CuO) [28]. Therefore, the electrodeposited metallic nanoparticles are consist of the inner Cu core and the outer CuO shell [29], and By considering the results of XRD analysis, Cu core atoms form a dominant cubic crystal structure. However, the electrochemical properties are affected by the nanostructured surface and the metal oxide. The rGO effect is unfolded in comparison between the CV curves of GCE and rGO/GCE, and CV curves of Cu NPs/GCE and Cu NPs/rGO/GCE. These observations reveal the rGO enhances the background current in rGO/GCE toward GCE, and increases peak current and decrease the peak potential separation of Cu NPs/rGO/GCE toward Cu NPs/GCE. It is associated with the high planar edge density of graphene layers and its porous structure which indicated the substantial edge plane coverage of rGO surface and increases the sites available for fast electron transfer in electrochemical reactions [30, 31]. Moreover, rGO nanosheets act as a conducting unit to enhance electronic conductivity [32, 33].

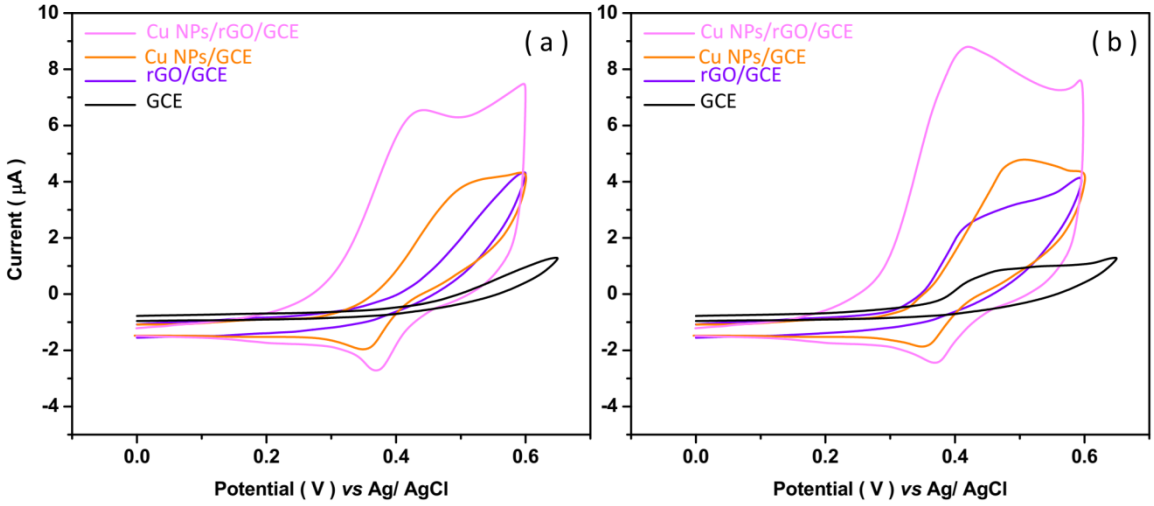

Figure 3. CV curves of GCE, rGO/GCE, Cu NPs/GCE and Cu NPs/rGO/GCE in 0.1 M Na_2SO_4 pH 7at scanning rate of 10 mV/s (a) without and (b) with 50 µM DCS.

Figure 3b displays the CV curves of GCE, rGO/GCE, Cu NPs/GCE and Cu NPs/rGO/GCE in 0.1 M Na_2SO_4 pH 7 containing 50 µM DCS solution at scanning rate of 10 mV/s. It can observe the anodic peak is observed on GCE and rGO/GCE at a potential of 0.45 V and 0.42 V, respectively,

demonstrating to oxidation of DCS. The suggested oxidation mechanism is 2-Hydroxyphenylacetic acid as primary products of the electro-oxidation of diclofenac, and 2,6-dichloroaniline that it oxidizes with the formation of 2,6-dihydroquinine [34] (Figure 4). The peak current of rGO/GCE is two times higher than that GCE due to high electrical conductivity, good hydrophobicity and large effective surface area of rGO with plenty of the oxygen-containing functional groups, and highly negative charged groups which correlated with the electrostatic interaction of rGO modified electrode with the positively charged DCS ions in solution [35, 36]. The CV curves of Cu NPs/GCE and Cu NPs/rGO/GCE show the oxidation peaks at 0.48 V and 0.41 V, respectively. The peak current of Cu NPs/rGO/GCE is two times and three times higher than that Cu NPs/GCE and rGO/GCE, respectively. Accordingly, the lower potential peak and the higher peak current are observed for Cu NPs/rGO/GCE. In addition, observation indicates to great role of electrodeposited Cu NPs in the enhancement of redox activity because the Cu species act as an active oxidizer to oxidation of analytes on the nanostructured electrode surface [35]. The synergetic effect of Cu NPs and rGO facilitates the electron transfer between the electrode and the electroactive species in solution and improves electrocatalytic oxidation of DCS. Therefore, the following electrochemical studies were carried out with Cu NPs/rGO/GCE.

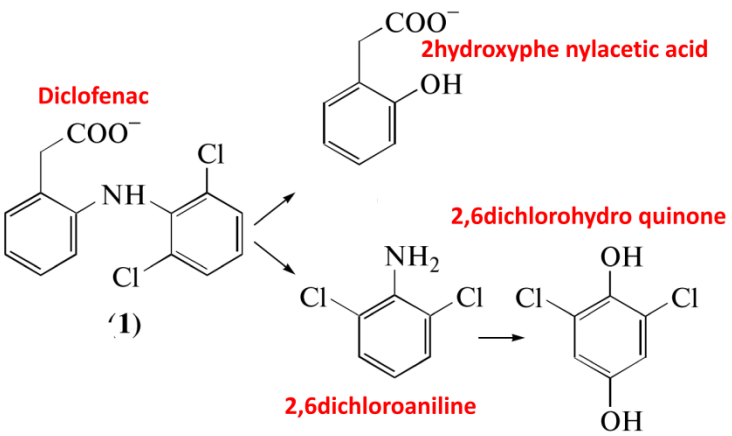

Figure 4. Oxidation mechanism of diclofenac

Figure 5 shows the amperometric response of Cu NPs/rGO/GCE to addition 50 µM DCS solution in0.1 M Na_2SO_4 pH 7 with speed rotation of 1000 rpm at the potential of 0.41 V. It is observed that there are fast responses and increase amperometric current after addition 10 µM DCS at 100^{th} s. The study of the stability of electrocatalytic response from 100^{th}s to 700^{th}s presents the decrease of 5% of amperometric current, illustrating the high stability of response of proposed electrode to determination of DCS that it is related to high mechanical and chemical stability of Cu NPs/rGO due to oxygenated functional groups on rGO surface and resulted in highly negative charge density [35, 37, 38], which can effectively bind the Cu ions to form the metal nanoparticles on the rGO surface via electrostatic interactions and provide the stable electroactive site on Cu NPs/rGO/GCE surface.

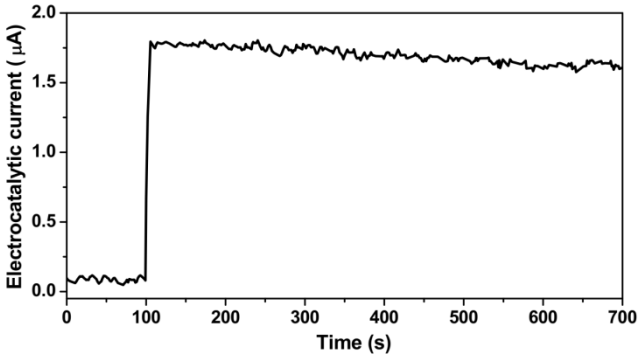

Figure 5. Amperometric response of Cu NPs/rGO/GCE to addition 50 µM DCS solution in 0.1 M Na_2SO_4 pH 7 with speed rotation of 1000 rpm at potential of 0.41 V.

Figure 6a shows the electrocatalytic response of electrode to successive additions of 20 µM DCS solution in 0.1 M Na_2SO_4 pH 7 at potential of 0.41 V. as seen, the amperometric current is increased after the addition of the DCS solution in an electrochemical cell. Figure 6b depicts the resulted calibration plot that it is evidence of a linear relationship between the electrocatalytic current and DCS concentration. The linear range, the limit of detection and sensitivity are obtained 20 to 400 µM, 8nM, and 0.0356µA/µM, respectively. Table 1 shows the performance of Cu NPs/rGO/GCE and other Cu and carbon nanostructured sensors in the literature for the determination of DCS.

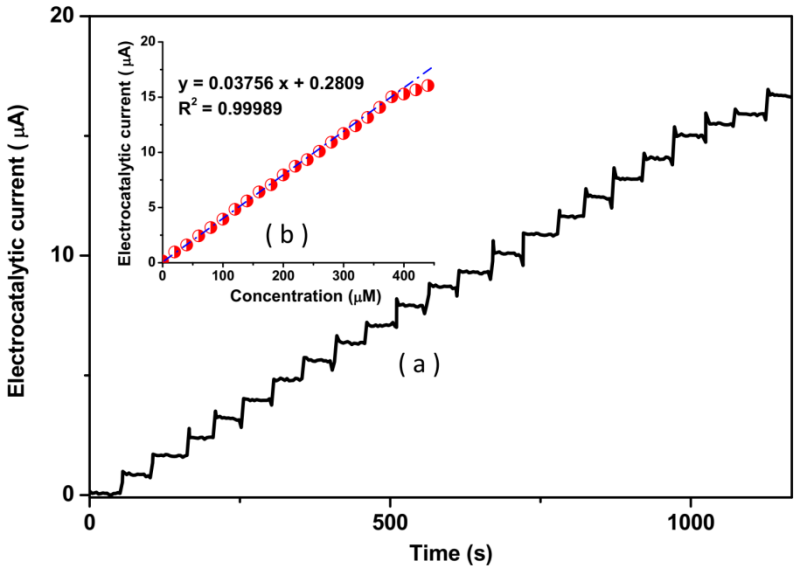

Figure 6. (a) Amperometric response of Cu NPs/rGO/GCE to successive additions of 20 µM DCS solution in 0.1 M Na_2SO_4 pH 7 with speed rotation of 1000 rpm at potential of 0.41 V; (b) Calibration plot.

Table 1. Performance of Cu NPs/rGO/GCE and other sensors in the literature for determination of DCS

Modified electrode	**Technique**	**Detection limit (nM)**	**Linear range (µM)**	**Ref.**
ionic liquid/CNTs paste electrode	DPV*	20	0.5–300	[39]
MWCNTs/Cu $(OH)_2$ NPs/hydrophobic ionic liquid 1-ethyl-3-methylimidazolium hexafluorophosphate/GCE	DPV	40	0.18–119	[40]
MWCNTs/Chitosan-Cu/GCE	SWV**	21	0.3 – 200	[41]
edge-plane pyrolytic graphite electrode	SWV	6.2	0.01–1	[42]
Nanocellulose/ f-MWCNTs/GCE	DPV	12	2–250	[43]
SWCNTs/edge-plane pyrolytic graphite electrode	SWV	22.5	0.025–1.5	[44]
Tyrosine/carbon paste electrode	CV	3280	10–140	[45]
ionic liquid/cobalt hexacyanoferrate NPs/MWCNTs	DPV	30	1–100	[46]
Au–Pt NPs/f-MWCNTs	DPV	300	0.5–1000	[47]
Cu-doped zeolite electrode	DPV	50	2.4–15	[48]
poly (diallyldimethylammonium chloride) functionalized graphene	DPV	609	10–100	[49]
Cu NPs/rGO/GCE	Amperometry	8	20-400	This work

*DPV: differential pulse voltammetry ** SWV:square wave voltammetry

It can be found that the electrocatalytic activity of Cu NPs/rGO/GCE was better than some others reported in the literature. In addition, the broad linear range and lowest detection limit of Cu NPs/rGO/GCE can be associated with π–π interaction between two twisted aromatic rings of diclofenac and rGO and Cu NPs [50].

Table 2 displays the results of a study of interference effect on the determination of DCS on Cu NPs/rGO/GCE using amperometry technique in 0.1 M Na_2SO_4 pH 7 at the potential of 0.41V under successive addition of 1 µM DCS and 4 µM of interfering species. As seen from Table 2, the amperometric current shows the significant signal for the addition of DCS, and inappreciable electrocatalytic current for addition of interfering species at 0.41 V that it represents the species in Table 2 don't show any interference with the determination of DCS by Cu NPs/rGO/GCE. Therefore, it is implied to excellent selectivity of prepared DCS sensor.

Table 2. Electrocatalytic current of Cu NPs/rGO/GCE using amperometry technique in 0.1 M Na_2SO_4 pH 7 at potential of 0.41 V under successive addition of 1 µM DCS and 7 µM of interfering species.

Substance	**Added (µM)**	Electrocatalytic current **(µA)**	**RSD (%)**
DCS	1	0.0381	±0.0011
K^+	7	0.0018	±0.0005
Mg^{2+}	7	0.0091	±0.0010
Ca^{2+}	7	0.0073	±0.0008
NH_4^+	7	0.0068	±0.0009
Br^+	7	0.0094	±0.0010
NO_3^-	7	0.0074	±0.0004
SO_4^{2-}	7	0.0087	±0.0008
Glucose	7	0.0077	±0.0009
Glycine	7	0.0095	±0.0010
Stearate	7	0.0077	±0.0008
Sucrose	7	0.0087	±0.0009
Ascorbic acid	7	0.0069	±0.0008
Dopamine	7	0.0058	±0.0007
Uric acid	7	0.0099	±0.0009
Urea	7	0.0097	±0.0009

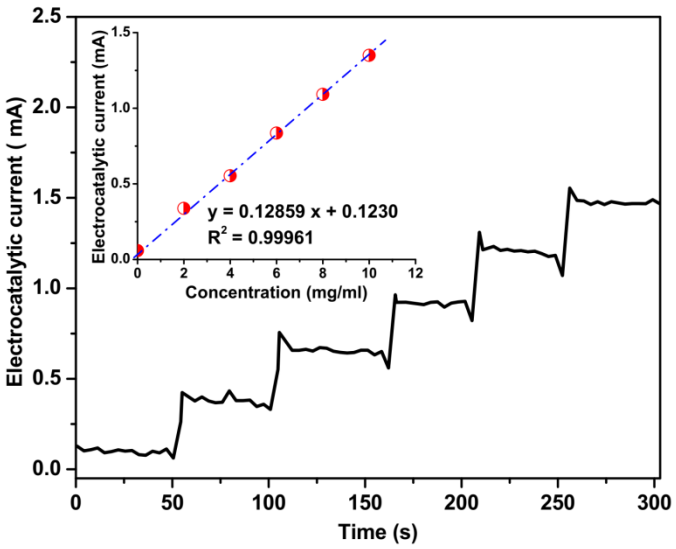

Figures 7. (a) Amperometry measurements of Cu NPs/rGO/GCE in prepared real pharmaceutical sample in 0.1 M Na_2SO_4 at potential of 0.41 V under successive addition of 2 mg/ml DCS; (b) Calibration plot.

For study the applicability of Cu NPs/rGO/GCE to determination DCS concentration in the prepared real pharmaceutical sample, the amperometry measurements was performed in the prepared real pharmaceutical sample in 0.1 M Na_2SO_4 potential of 0.41V under successive addition of 2mg/ml DCS. Figure 7 exhibits the obtained amperogramm and calibration plot. The calibration plot shows that the diclofenac concentration in the prepared sample is 0.957 mg/ml which is close to the1 mg/ml

diclofenac content and in agreement with the labeled value of tablets (25 mg per tablet). Table 3 shows the recovery and RSD of spiked levels in the prepared real pharmaceutical sample which indicated recovery (≥97.66%) and RSD (≤3.05%) values are acceptable and this method provides suitable precision and accuracy for practical analyses in pharmaceutical samples using Cu NPs/rGO/GCE.

Table 3. Recovery and RSD of spiked levels in prepared real pharmaceutical sample of diclofenac tablets.

Added (mg/ml)	**Found** (mg/ml)	**Recovery (%)**	**RSD (%)**
2.00	1.97	98.50	2.07
4.00	3.91	97.75	2.41
6.00	5.86	97.66	2.55
8.00	7.92	99.00	3.01
10.00	9.88	98.80	3.05

4. CONCLUSION

This work was carried out for synthesizing Cu NPs/rGO/GCE for electrochemical determination of DCS in the pharmaceutical samples. rGO nanosheets were synthesized by the modified Hummers method and Cu NPs were electrodeposited on rGO/GCE. Studies of the structure and morphology of nanostructures exhibited that the pore structure of rGO nanosheets and Cu NPs in the cubic crystal structure were synthesized. Electrochemical studies showed that linear range, the limit of detection, and sensitivity were obtained 20 to 400 µM, 8 nM, and 0.0356µA/µM, respectively for Cu NPs/rGO/GCE as DCS sensor. Study of applicability of Cu NPs/rGO/GCE to determination DCS concentration in the prepared real pharmaceutical sample that showed recovery (≥97.66%) and RSD (≤3.05%) values were acceptable and this method provided suitable precision and accuracy for practical analyses in pharmaceutical samples using Cu NPs/rGO/GCE.

References

1. A.J. Al-Rajab, L. Sabourin, D.R. Lapen and E. Topp, *Science of the Total Environment*, 409 (2010) 78.
2. W.-Y. Huang, G.-Q. Wang, W.-H. Li, T.-T. Li, G.-J. Ji, S.-C. Ren, M. Jiang, L. Yan, H.-T. Tang and Y.-M. Pan, *Chem*, 6 (2020) 2300.
3. X.-Q. Lin, Z.-L. Li, B. Liang, H.-L. Zhai, W.-W. Cai, J. Nan and A.-J. Wang, *Water research*, 162 (2019) 236.
4. H. Karimi-Maleh, Y. Orooji, F. Karimi, M. Alizadeh, M. Baghayeri, J. Rouhi, S. Tajik, H. Beitollahi, S. Agarwal and V.K. Gupta, *Biosensors and Bioelectronics*, 184 (2021) 113252.
5. P.A. Todd and E.M. Sorkin, *Drugs*, 35 (1988) 244.
6. Y. Duan, Y. Liu, Z. Chen, D. Liu, E. Yu, X. Zhang, H. Fu, J. Fu, J. Zhang and H. Du, *Green Chemistry*, 22 (2020) 44.

7. L.-F. Hsieh, C.-Z. Hong, S.-H. Chern and C.-C. Chen, *Journal of pain and symptom management*, 39 (2010) 116.
8. X. Wang, Z. Feng, B. Xiao, J. Zhao, H. Ma, Y. Tian, H. Pang and L. Tan, *Green Chemistry*, 22 (2020) 6157.
9. J. Zhang, M. Wang, Y. Tang, Q. Ding, C. Wang, X. Huang, D. Chen and F. Yan, *IEEE Transactions on Instrumentation and Measurement*, 70 (2021) 1.
10. Y. Orooji, B. Tanhaei, A. Ayati, S.H. Tabrizi, M. Alizadeh, F.F. Bamoharram, F. Karimi, S. Salmanpour, J. Rouhi and S. Afshar, *Chemosphere*, 281 (2021) 130795.
11. Z. Lei, S. Hao, J. Yang, L. Zhang, B. Fang, K. Wei, Q. Lingbo, S. Jin and C. Wei, *Chemosphere*, 270 (2021) 128646.
12. Z. Ni, X. Cao, X. Wang, S. Zhou, C. Zhang, B. Xu and Y. Ni, *Coatings*, 11 (2021) 749.
13. P. Daneshgar, P. Norouzi, M.R. Ganjali, R. Dinarvand and A.A. Moosavi-Movahedi, *Sensors*, 9 (2009) 7903.
14. P.M. Jahani, S.Z. Mohammadi, A. Khodabakhshzadeh, J.H. Cha, M.S. Asl, M. Shokouhimehr, K. Zhang, Q. Van Le and W. Peng, *International Journal of Electrochemical Science*, 15 (2020) 9037.
15. S. Thiagarajan, M. Rajkumar and S.-M. Chen, *International Journal of Electrochemical Science*, 7 (2012) 2109.
16. R. Farghali, R.A. Ahmed and A.A. Alharthi, *International Journal of Electrochemical Science*, 13 (2018) 10390.
17. H. Karimi-Maleh, M.L. Yola, N. Atar, Y. Orooji, F. Karimi, P.S. Kumar, J. Rouhi and M. Baghayeri, *Journal of colloid and interface science*, 592 (2021) 174.
18. Z. Savari, S. Soltanian, A. Noorbakhsh, A. Salimi, M. Najafi and P. Servati, *Sensors and Actuators B: Chemical*, 176 (2013) 335.
19. L. Zhang, J. Zheng, S. Tian, H. Zhang, X. Guan, S. Zhu, X. Zhang, Y. Bai, P. Xu and J. Zhang, *Journal of Environmental Sciences*, 91 (2020) 212.
20. H. Savaloni, E. Khani, R. Savari, F. Chahshouri and F. Placido, *Applied Physics A*, 127 (2021) 1.
21. Y. Yang, H. Chen, X. Zou, X.-L. Shi, W.-D. Liu, L. Feng, G. Suo, X. Hou, X. Ye and L. Zhang, *ACS applied materials & interfaces*, 12 (2020) 24845.
22. G. Huang, C. Lv, J. He, X. Zhang, C. Zhou, P. Yang, Y. Tan and H. Huang, *Journal of Nanomaterials*, 2020 (2020) 2042316.
23. A.T. Smith, A.M. LaChance, S. Zeng, B. Liu and L. Sun, *Nano Materials Science*, 1 (2019) 31.
24. K.H. Kim, M. Yang, K.M. Cho, Y.-S. Jun, S.B. Lee and H.-T. Jung, *Scientific reports*, 3 (2013) 1.
25. Z. Protich, K. Santhanam, A. Jaikumar, S. Kandlikar and P. Wong, *Journal of The Electrochemical Society*, 163 (2016) E166.
26. S. Giri and A. Sarkar, *Journal of The Electrochemical Society*, 163 (2016) H252.
27. W. Gu, M. Wang, X. Mao, Y. Wang, L. Li and W. Xia, *Analytical Methods*, 7 (2015) 1313.
28. Y. Wu, X. Chen, D. Huang, L. Zhang, Y. Ren, G. Tang, X. Chen, B. Yue and H. He, *Catalysis Science & Technology*, 10 (2020) 3985.
29. X. Zhang, X. Zhou, Y. Guo, J. Li, C. Hu, K. Zhang and L. Wang, *Nanotechnology*, 32 (2021) 095707.
30. A. García-Miranda Ferrari, D.A.C. Brownson and C.E. Banks, *Scientific Reports*, 9 (2019) 15961.
31. F. Chahshouri, H. Savaloni, E. Khani and R. Savari, *Journal of Micromechanics and Microengineering*, 30 (2020) 075001.
32. S. Al-Rubaye, R. Rajagopalan, S.X. Dou and Z. Cheng, *Journal of Materials Chemistry A*, 5 (2017) 18989.

33. L. Zhang, M. Zhang, S. You, D. Ma, J. Zhao and Z. Chen, *Science of The Total Environment*, 780 (2021) 146505.
34. M. Vedenyapina, D. Borisova, K.-H. Rosenwinkel, D. Weichgrebe, P. Stopp and A. Vedenyapin, *Russian Journal of Physical Chemistry A*, 87 (2013) 1393.
35. S. Phetsang, P. Kidkhunthod, N. Chanlek, J. Jakmunee, P. Mungkornasawakul and K. Ounnunkad, *Scientific Reports*, 11 (2021) 9302.
36. W. Peng, H. Li, Y. Liu and S. Song, *Journal of Molecular Liquids*, 230 (2017) 496.
37. R. Sitko, E. Turek, B. Zawisza, E. Malicka, E. Talik, J. Heimann, A. Gagor, B. Feist and R. Wrzalik, *Dalton transactions*, 42 (2013) 5682.
38. H. Karimi-Maleh, S. Ranjbari, B. Tanhaei, A. Ayati, Y. Orooji, M. Alizadeh, F. Karimi, S. Salmanpour, J. Rouhi and M. Sillanpää, *Environmental Research*, 195 (2021) 110809.
39. A.A. Ensafi, M. Izadi and H. Karimi-Maleh, *Ionics*, 19 (2013) 137.
40. M. Arvand, T.M. Gholizadeh and M.A. Zanjanchi, *Materials Science and Engineering: C*, 32 (2012) 1682.
41. M. Shalauddin, S. Akhter, S. Bagheri, M.S. Abd Karim, N. Adib Kadri and W.J. Basirun, *International Journal of Hydrogen Energy*, 42 (2017) 19951.
42. R.N. Goyal, S. Chatterjee and B. Agrawal, *Sensors and Actuators B: Chemical*, 145 (2010) 743.
43. M. Shalauddin, S. Akhter, W.J. Basirun, S. Bagheri, N.S. Anuar and M.R. Johan, *Electrochimica Acta*, 304 (2019) 323.
44. R.N. Goyal, S. Chatterjee and A.R.S. Rana, *Carbon*, 48 (2010) 4136.
45. B.K. Chethana, S. Basavanna and Y. Arthoba Naik, *Industrial & Engineering Chemistry Research*, 51 (2012) 10287.
46. S. Damiri, Y.M. Oskoei and M. Fouladgar, *Journal of Experimental Nanoscience*, 11 (2016) 1384.
47. M.M. Eteya, G.H. Rounaghi and B. Deiminiat, *Microchemical Journal*, 144 (2019) 254.
48. F. Manea, M. Ihos, A. Remes, G. Burtica and J. Schoonman, *Electroanalysis*, 22 (2010) 2058.
49. O.K. Okoth, K. Yan, L. Liu and J. Zhang, *Electroanalysis*, 28 (2016) 76.
50. J. Rashid, F. Saleemi, B. Akram, L. Wang, N. Hussain and M. Xu, *Nanomaterials*, 11 (2021) 1564.